

Growth-kinetics-induced structural disorder in $\text{Bi}_2(\text{Sr}_{1-x}\text{Ca}_x)_3\text{Cu}_2\text{O}_y$ thin films studied by x-ray diffraction

A. Vailionis, A. Brazdeikis, and A. S. Flodström

Department of Physics, Materials Physics, Royal Institute of Technology, S-10044 Stockholm, Sweden

(Received 5 July 1994)

Thin films of $\text{Bi}_2(\text{Sr}_{1-x}\text{Ca}_x)_3\text{Cu}_2\text{O}_y$ grown *in situ* by molecular-beam epitaxy have been studied by x-ray diffraction. The experimental results were interpreted using a general one-dimensional kinematic x-ray-diffraction model. An accurate determination of the lattice structure and of the distribution of the different atoms on the lattice sites is obtained. The model uniquely reconstructs a large substitution between Ca^{2+} and Sr^{2+} at the Ca and Sr lattice sites. The model also predicts an expansion of the $\text{CuO}_2\text{-CuO}_2$ and a contraction of the SrO-CuO₂ interplanar distances compared with x-ray-diffraction data reported from bulk single crystals. The large atomic substitution between different lattice sites is attributed to the growth kinetics, which for molecular-beam epitaxy plays a major role in forming the growing epitaxial structure, due to the low interaction energy between the thermal atom beams and the substrate surface inherent to the molecular-beam epitaxy process. This structural disorder is interpreted as causing the suppressed superconducting transition temperatures, T_c 's and the broad superconducting transition widths, ΔT_c 's observed for $\text{Bi}_2(\text{Sr}_{1-x}\text{Ca}_x)_3\text{Cu}_2\text{O}_y$ films grown by molecular-beam epitaxy compared with films fabricated by magnetron sputtering or laser ablation. The relation between the structural disorder and the superconducting properties is discussed.

I. INTRODUCTION

The discovery of superconductivity in the Bi-Sr-Ca-Cu-O system¹ initiated structural studies which revealed the presence of CuO_2 planes as a common feature of this class of high- T_c cuprate superconductors.²⁻⁴ Because of possible differences in the copper coordination within the planes as well as differences in the interlayer coupling between them, both of which are important for the superconductivity,⁵ a knowledge of the structural disorder caused by cationic substitution in these compounds and its consequences for the lattice structure is important. The Bi-based cuprates with the generic formula $\text{Bi}_2\text{Sr}_2\text{Ca}_{n-1}\text{Cu}_n\text{O}_y$ have strongly anisotropic layered structures that are composed of stacked planes of BiO, SrO, CuO_2 , and Ca. The stacking order of the planes can lead to a variety of superconducting phases characterized by the number of CuO_2 and Ca planes in the unit cell. The phase responsible for the $T_c \approx 80$ K superconductivity is known to have the composition $\text{Bi}_2(\text{Sr}_{1-x}\text{Ca}_x)_3\text{Cu}_2\text{O}_{8+\delta}$, the ideal composition being $\text{Bi}_2\text{Sr}_2\text{CaCu}_2\text{O}_{8+\delta}$ (Bi-2212). The superconducting current in the Bi-2212 phase is carried by the two two-dimensional CuO_2 planes in each half of the unit cell and the Bi_2O_2 layers act as the necessary reservoirs providing the superconducting carriers.^{6,7} Sr^{2+} and Ca^{2+} ions are known to substitute for each other without causing changes in the lattice structure or precipitation of secondary phases in the Bi-2212 compound.^{8,9} Such substitutions do not affect the formal valency of the copper, but they are expected to push apart adjacent CuO_2 planes due to differences in ionic radii. Substitutions may also occur in the BiO planes, where Bi^{3+} ions can be replaced by Ca^{2+} and/or Sr^{2+} .^{3,10} The importance of these substitu-

tions on the superconductivity in the Bi-based cuprates is not clear and needs to be further investigated. There are other aspects that have been studied for bulk materials that need to be examined for epitaxial high- T_c thin films. In contrast to ordinary bulk synthesis, thin-film synthesis is not a thermodynamic equilibrium process, and it is expected that growth kinetics will play a major role in the formation of the films. The synthesis of highly metastable phases which cannot be obtained as bulk materials as well as the site-selective doping of CuO_2 planes become possible by epitaxial thin-film synthesis. In fact, the preparation conditions may drastically affect the structural properties of the films. The substitutional disorder may agglomerate and negatively affect the superconducting properties. However, if properly understood, the effects may also be used to accomplish positive goals such as the enhancement of thin-film device performance or process yields. The understanding of these relationships needs a comprehensive analysis. The intention of the present study has been to investigate the structural disorder induced in $\text{Bi}_2(\text{Sr}_{1-x}\text{Ca}_x)_3\text{Cu}_2\text{O}_y$ thin films due to the growth kinetics. For this purpose, a general one-dimensional kinematic x-ray-diffraction (XRD) model commonly used for the study of superlattice structures¹¹ was extended and applied to $\text{Bi}_2(\text{Sr}_{1-x}\text{Ca}_x)_3\text{Cu}_2\text{O}_y$.

II. EXPERIMENT

Films were grown by molecular-beam epitaxy (MBE) using a technique described in detail elsewhere.¹² Thin films of the Bi-2212 crystal structure were formed by *in situ* oxidation of the evaporated metallic components on (100)-oriented MgO substrates at temperatures of 690 °C. Typical film thicknesses were about 30 nm. After the

MBE growth, the surface crystallography was studied by *in situ* reflection high-energy electron diffraction (RHEED). XRD analysis was used to verify the quality of epitaxy, to determine the *c*-axis lattice parameter, and to study the phase purity of the films. XRD spectra were recorded using a Siemens D5000 x-ray diffractometer in the Bragg-Brentano geometry using Cu $K\alpha$ radiation ($\lambda = 1.5406 \text{ \AA}$). The ultimate resolution was $\Delta\Theta = 0.02^\circ$. A separate alignment correction was made for each sample. Chemical compositions were obtained from energy dispersive x-ray spectroscopy. The electrical resistivity was measured using a conventional four-probe method and applying the $1\text{-}\mu\text{V/cm}$ criterion.

The one-dimensional kinematic x-ray-diffraction model used in the present study was developed for superlattices and for Y-Ba-Cu-O superconducting thin films by Fullerton *et al.*¹¹ A detailed mathematical formalism of the model adapted to the Bi-2212 structure is given in the Appendix. Briefly, the unit-cell structure of Bi-2212 is layered and composed of stacked planes of BiO, SrO, CuO₂, and Ca, as shown in Fig. 1. For the model calculations, the layer sequence of half the unit cell is written as -BiO-SrO-CuO₂-Ca-CuO₂-SrO-BiO-. Figure 2 illustrates a Bi-2212 film which is represented as a superlattice with M stacked bilayers of BiO, SrO, CuO₂, and single Ca planes. The spacing between r and $(r+1)$ planes in the j th layer is $d_{r,j}$. Each layer is separated by a BiO-BiO distance $d_{\text{Bi},j}$. The r th plane of the j th layer is characterized by the scattering power $f_{r,j}(q)$. All corrections, such as

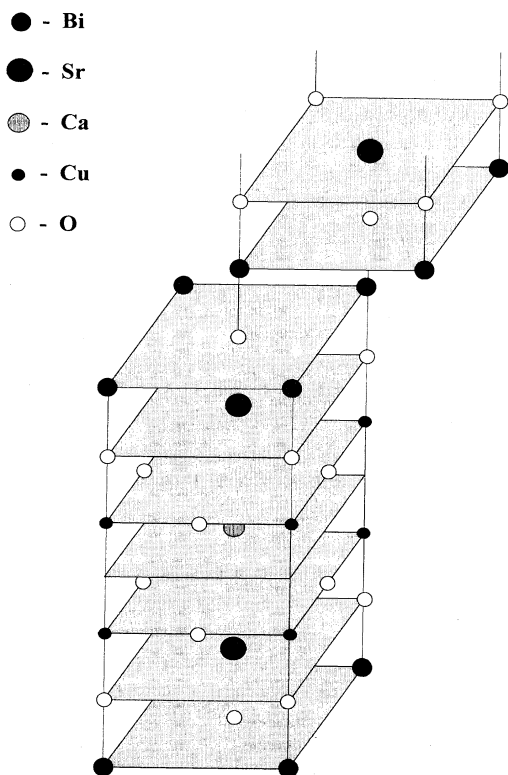


FIG. 1. The crystal structure of Bi₂Sr₂CaCu₂O₈ phase which consists of the BiO, SrO, CuO₂, and Ca planes (schematic).

Debye-Waller coefficient, Lorentz-polarization, and absorption factors, are included. Since the measured XRD profiles exhibited Gaussian-type peak shapes, only a Gaussian distribution function was involved in the model to refine the structure. The structure factor and the total scattering intensity calculations are presented in the Appendix. The interplanar distances between BiO, SrO, and CuO₂ planes and the in-plane atomic substitutions of Bi, Sr, and Ca were used as fitting parameters.

III. RESULTS

In situ recorded RHEED images showed a clear two-dimensional surface pattern with the incommensurate modulation and 90°-oriented grain boundaries along [100] and [110] azimuth of the MgO (100) substrate.¹² $T_{c,\text{zero}}$ of 65–75 K with superconducting transition onset temperatures at 80 K were routinely achieved. The full width at half maximum of the (0010) rocking curves was in all cases close to 0.3°. The diffraction data reflect the high quality of the out-of-plane epitaxy of the films. The *c*-axis lattice parameter was for all the samples close to 30.8 Å, identical to that observed for bulk Bi-2212. For some films, weak impurity peaks originating from CuO (111) plane diffraction appeared in the XRD scans. High-resolution electron microscopy (HREM) studies

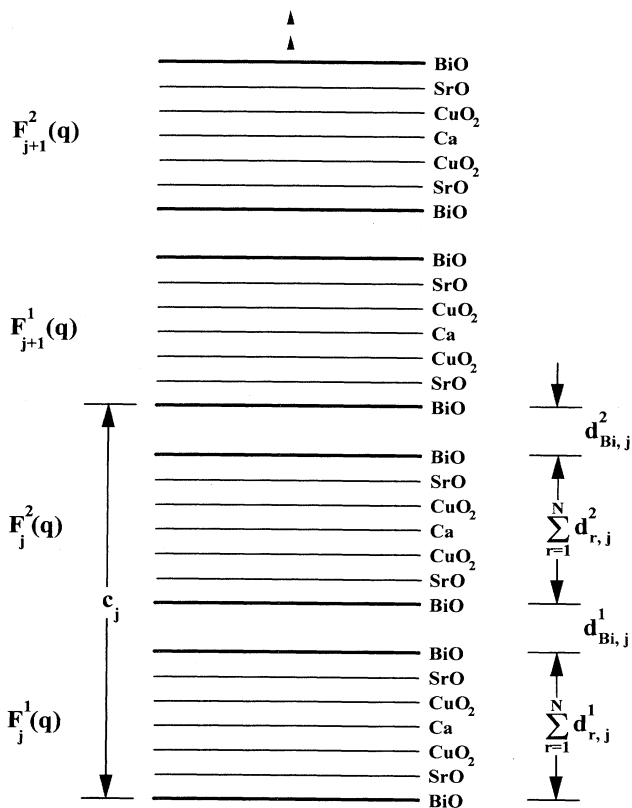


FIG. 2. Model of Bi-2212 thin film represented as a superlattice. The j th bilayer includes two half unit cells with structure factors $F_j^1(q)$ and $F_j^2(q)$. Each layer is separated by BiO-BiO distances $d_{\text{Bi},j}$. The thickness of the bilayer is equal to the unit-cell length c_j .

confirmed the RHEED data concerning the incommensurate modulations along the [110] direction and the a - b plane twinning.¹³ Stacking faults in which some layers of $-\text{CuO}_2\text{-Ca-CuO}_2-$ were replaced by layers of $-\text{CuO}_2\text{-Ca-CuO}_2-$ (2223) and/or $-\text{CuO}_2-$ (2201) were observed only rarely in the HREM images. The fitting of XRD profiles implied that the number of stacking faults was less than 10% in all the samples investigated. In fact, both XRD data and HREM cross-sectional images showed that the CuO-rich impurities appear only as isolated surface precipitates or localized at the substrate-film interface, and in both cases only at a low volume fraction. Neither the small quantities of impurity precipitates nor the low density of stacking faults is believed to influence the superconducting properties, i.e., the depressed T_c 's or the broad superconducting transitions of the films.

A calculated XRD spectrum of a Bi-2212 film with a thickness of 10 unit cells using atomic positions obtained from bulk Bi-2212 single crystals³ (hereafter denoted as "ideal") is shown in Fig. 3(a). The comparison between calculated and measured XRD spectra was performed only for high diffraction angles due to the limitations of

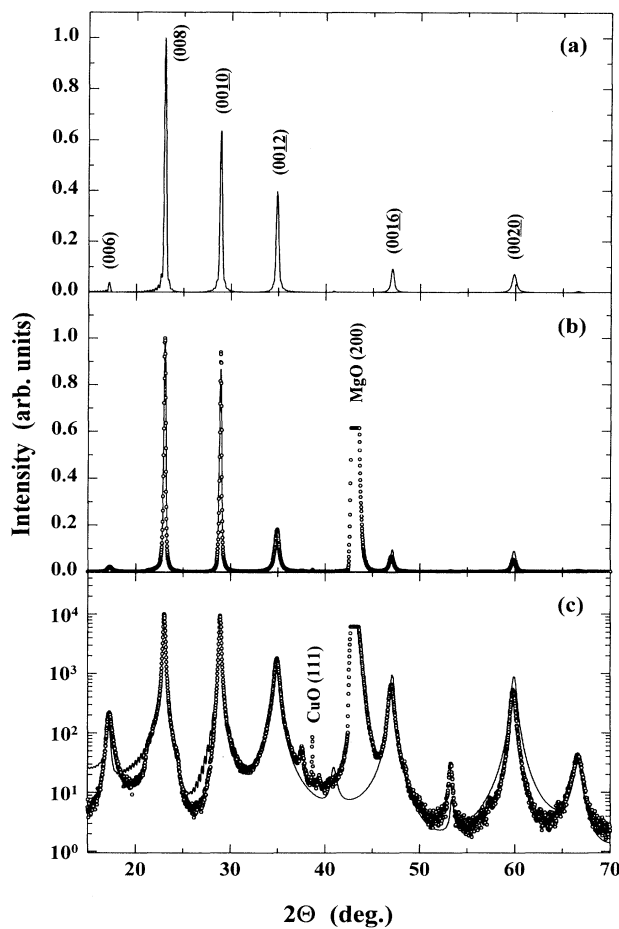


FIG. 3. Measured (open circles) and calculated (solid lines) x-ray-diffraction profiles of Bi-2212 thin film: (a) "ideal" film consisting of $M=10$ unit cells, refined spectra of the No. 166 sample on (b) a linear and (c) a logarithmic scale. All profiles are normalized to the (008) peak intensity.

the kinematic model for low diffraction angles. Figures 3(b) and 3(c) display the measured XRD spectra of the No. 166 sample (open circles) and the corresponding fitted spectra (solid lines) on a linear and logarithmic scale, respectively. The peak positions, the relative intensities and the linewidths of the measured XRD spectrum are reproduced quite well. To fit the experimental profile, continuous interplanar distance fluctuations around 0.04 Å as well as the presence of 3.5% of Bi-2201 and 4.6% of Bi-2223 structures as stacking faults are required.¹⁴ As can readily be seen in Figs. 3(a) ("ideal") and 3(b) (experimental), there are a number of discrepancies in the relative peak intensities between the experimental and the "ideal" spectra. In particular, the (0012) peak intensity is suppressed in relation to the (0010) peak intensity in the experimental data compared with the simulated "ideal" x-ray-diffraction spectrum. The quoted and displayed structural features are typical among the large number of samples grown in the same way and are generally valid for MBE-grown films. According to the simulations, the interplanar $\text{CuO}_2\text{-CuO}_2$ distances should be expanded from 3.3 to 3.4 Å and the SrO-CuO_2 distances should be contracted from 1.7 to 1.6 Å compared with the "ideal" positions in the bulk Bi-2212 single crystals. The Ca sites must be partly populated by Sr^{2+} ions, and the Sr sites must be partly populated by Bi^{3+} and/or Ca^{2+} ions, see Table I.

IV. DISCUSSION

In general, the MBE-grown, Bi-based cuprate films exhibit somewhat lower T_c 's and broader transition widths, ΔT_c 's than the magnetron-sputtered or laser-ablated films.¹⁵ The broad superconducting transition of Bi-based thin films has often been associated with the presence of stacking faults,^{16,17} nonuniform oxygenation,^{15,18} unintentional molybdenum contamination,^{19,20} or cationic nonstoichiometry.^{17,21} It is apparent from both HREM and XRD data that the density of stacking faults is quite low and it therefore seems improbable that stacking faults or phase intergrowths cause the large ΔT_c 's transitions. Low-temperature annealing experiments²² prove that the large ΔT_c 's cannot originate from nonuniform oxygenation. Molybdenum or cationic nonstoichiometry are also discarded. Thus it seems that for the large ΔT_c 's in the MBE-grown films other factors must be considered besides those earlier proposed. It is suggested that the broad superconducting transition in the MBE-grown Bi-2212 thin films is caused by structural disorder, due to the large substitutions between Sr and Ca in the lattice.

TABLE I. Refined site occupancies of MBE-grown Bi-2212 thin films. Single-crystal data are taken from (Ref. 3).

	Bi site			Sr site			Ca site		
	Bi	Sr	Ca	Bi	Sr	Ca	Bi	Sr	Ca
Single crystal	0.99	0.00	0.00	0.05	0.86	0.00	0.06	0.19	0.75
No. 166	1.00	0.00	0.00	0.14	0.65	0.21	0.00	0.52	0.48
No. 167	1.00	0.00	0.00	0.18	0.59	0.23	0.20	0.24	0.56
No. 177	1.00	0.00	0.00	0.13	0.61	0.26	0.00	0.63	0.37

The structural disorder leads to changes in the interplanar distances in the unit cell that severely influence the superconducting properties.

The discrepancy in peak intensities observed between the measured and the "ideal" XRD spectra implies a greater disorder in the structure of MBE-grown thin films than in bulk materials. The large degree of substitution between Ca^{2+} and Sr^{2+} cause the $\text{CuO}_2\text{-CuO}_2$ interplanar distance to increase. The deduced Ca and Sr site occupancies are shown in Table I. The plot in Fig. 4 represents the calculated intensity of the (0012) peak as a function of the $\text{CuO}_2\text{-CuO}_2$ interplanar distance. The significantly suppressed peak intensity, as much as 20%, can be reproduced only if the $\text{CuO}_2\text{-CuO}_2$ distance is substantially increased. If a contraction of the SrO-SrO interplanar distance is introduced to keep the c -axis lattice parameter constant, as deduced from the experimental XRD spectra, this intensity suppression becomes less. The other high intensity Bragg peaks, e.g., the (0010), (0016), and (0020) peaks, were found to be almost independent of the quoted changes in the interplanar distances. The expansion of the $\text{CuO}_2\text{-CuO}_2$ interplanar distance can be understood in terms of substitutions in the Ca plane of Ca^{2+} ions by the larger Sr^{2+} ions. Such a substitution does not affect the valency of the copper. The increase in the $\text{CuO}_2\text{-CuO}_2$ interplanar distance induces a contraction in the SrO-SrO interplanar distance, while the c -axis lattice parameter remains constant (see Table II). In contrast to bulk Bi-2212 materials,^{4,9} the MBE-grown thin films show a larger degree of substitution between Sr and Ca. The large substitutions in the MBE-grown films and the resulting disorder are probably related to an incomplete ordering of the adatoms during film formation. It is known that the film growth does not

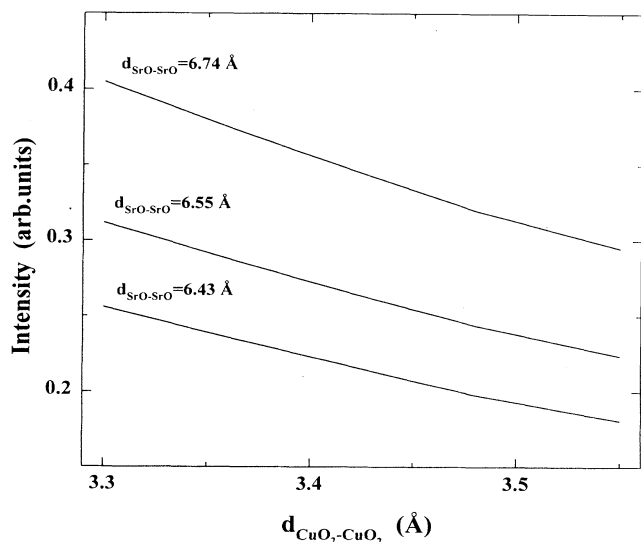


FIG. 4. Calculated intensity of the (0012) peak of Bi-2212 thin film consisting of $M=10$ unit cells as a function of the $\text{CuO}_2\text{-CuO}_2$ interplanar distance with different distances between the SrO-SrO planes. The intensity is normalized to the (008) peak intensity.

TABLE II. Refined interplanar distances (Å) of Bi-2212 thin films. Unit-cell lengths were calculated from x-ray-diffraction spectra. R_{wp} is defined as $(\sum_j w_j [I_{oj} - I_{cj}]^2 / \sum_j w_j I_{oj}^2)^{1/2}$, where I_{oj} and I_{cj} are the observed and calculated intensities, respectively, and w_j is the weighting factor determined as $1/I_{oj}$.

	Unit-cell length	BiO-SrO	SrO-CuO ₂	CuO ₂ -Ca	R_{wp}
Single crystal	30.87	2.73	1.72	1.65	
No. 166	30.84	2.79	1.57	1.71	0.28
No. 167	30.84	2.85	1.58	1.70	0.32
No. 177	30.83	2.80	1.58	1.71	0.30

take place at thermodynamic equilibrium. The arrangement of atoms in the unit cell is controlled by the growth kinetics. In a two-dimensional picture, the atoms are at first physisorbed on impact with the substrate surface. The low binding energy of the adatoms in the physisorbed state means that they easily move over the surface. Before the final "correct" chemisorbed state is reached, the atoms may choose "wrong" chemisorption sites or form intermediate chemical states of stable binary or ternary oxides in the form of clusters. Under these circumstances, the transformation to the final "correct" chemisorption state may even require reallocation of the cluster atoms and therefore substantially more energy. In the MBE synthesis, the kinetic energies of the depositing species upon impact with the substrate at a given temperature T are between kT_{source} and kT , a very small energy. Thus the adatoms in the "wrong" and/or intermediate chemisorbed states are for kinetic reasons hindered, from a thermodynamic viewpoint, from moving to energetically more favorable configurations. This may cause disorder in the form of differently occupied sites for Sr and Ca in the unit cell of Bi-2212. In the magnetron sputter and laser-ablation processes, ions and neutral particles hitting the surface have kinetic energies far greater than kT , which will supply "extra" energy to the surface and help proper ordering. The role of the growth kinetics for the observed disorder and the relation between disorder and the measured physical properties of the MBE-grown thin films are still not very clear and thus need to be investigated further.

The atomic displacement may give a rise to an inhomogeneous strain (microstrain) in the thin film observed as an additional broadening of the x-ray-diffraction peaks.^{23,24} This type of broadening is derived from a variation in d spacing in the direction considered and usually tends to be Gaussian.²⁴ The distortions due to microstrain in the lattice of the $\text{Bi}_2(\text{Sr}_{1-x}\text{Ca}_x)_3\text{Cu}_2\text{O}_y$ films contribute to continuous interplanar distance fluctuations as previously mentioned and appear as a part of the Gaussian broadening of the XRD profile. According to the fitting results, the Lorentzian (Cauchy) component of the line profile, which arises due to a small domain size, was not identified.

It is important to understand how the changes in the Cu local atomic coordination may affect the superconducting properties of the Bi-based cuprates. For high- T_c bulk materials with $T_c \geq 100$ K such as $\text{HgBa}_2\text{CaCu}_2\text{O}_y$,

(Hg-1212) and $\text{Ti}_2\text{Ba}_2\text{CaCu}_2\text{O}_8$ (Ti-2212), the interplanar CuO_2 - CuO_2 distances are 3.15 and 3.20 Å, respectively,^{25,26} compared to 3.30 Å for Bi-2212. The increase in the CuO_2 - CuO_2 interplanar distance is an important parameter expected to influence the superconducting properties of high- T_c materials. On the other hand, the oxygen in the SrO plane is related to the CuO_5 pyramid as apex oxygen. Therefore, the reduction in the SrO- CuO_2 interplanar distance moves the oxygen together with the Sr^{2+} ion closer to the Cu atom. In Hg-1212 and Ti-2212 compounds, the distance between the Cu and the apex oxygen is 2.74 Å,^{25,26} whereas it is only 2.50 Å for Bi-2212. The bond length between the Cu and the apex oxygen is known to determine the degree of two-dimensionality of the CuO_2 planes. The longer bond length suggests a stronger two dimensionality of the CuO_2 planes and is essential for the cuprates with $T_c \geq 100$ K.

V. CONCLUSIONS

The lattice structure of Bi-2212 thin films grown by MBE was determined from experimental x-ray-diffraction spectra by a fitting procedure using a one-dimensional kinematic x-ray-diffraction model. Interplanar distances and atomic substitutions within the unit cell were used as parameters in fitting the experimental spectra. The interplanar CuO_2 - CuO_2 distances were found to be expanded from 3.3 to 3.4 Å and the SrO- CuO_2 distances were found to be contracted from 1.7 to 1.6 Å. It was shown that the changes can be related to large substitutions

mainly between Sr^{2+} and Ca^{2+} ions at the Ca and Sr sites. The origin of these substitutions is interpreted as being caused by incomplete ordering of the adatoms during film growth. The structural disorder results in a suppressed T_c and a broad superconducting transition, ΔT_c , for MBE-grown films compared with bulk materials or thin films synthesized by magnetron sputtering and laser ablation. Experiments to investigate the correlation between the structural features and the transport and magnetic properties of the films should be performed. Work is in progress to determine the interatomic distances in the unit cell for the MBE-synthesized thin films by extended x-ray-absorption fine structure.

ACKNOWLEDGEMENTS

We thank Professor Y. Bruynseraede, Katholieke Universiteit Leuven for providing the SUPREX program. This work was supported by the Swedish Research Council for Engineering Sciences (TFR) and the Swedish National Board for Industrial and Technical Development (NUTEK).

APPENDIX

The one-dimensional structure factor $F(q)$ for Bi-2212 film which is described as a superlattice with M stacked bilayers of BiO, SrO, CuO_2 , and single Ca planes (see Fig. 2) including cumulative interplanar distances fluctuations can be written as

$$F(q) = \sum_{j=1}^M \exp(iqc_j) \left[F_j^1 + \exp \left[iq \left[\sum_{r=1}^{N-1} d_{r,j}^1 + d_{\text{Bi},j}^1 \right] \right] F_j^2 \right], \quad (\text{A1})$$

where $q = 4 \sin\Theta / \lambda$ is the scattering vector, $d_{r,j}$ and $d_{\text{Bi},j}$ are the distances between r -($r+1$) and BiO-BiO planes, respectively, N is the number of planes in the layer and c_j is the thickness of the j th bilayer given by

$$c_j = \sum_{r=1}^{N-1} (d_{r,j}^1 + d_{r,j}^2) + d_{\text{Bi},j}^1 + d_{\text{Bi},j}^2, \quad (\text{A2})$$

F_j^1, F_j^2 are structure factors of the j th bilayer defined by

$$F_j^1(q) = \sum_{k=1}^N f_k \left[iq \sum_{r=1}^{k-1} d_{r,j}^1 \right], \quad (\text{A3})$$

$$F_j^2(q) = \sum_{k=1}^N f_k \left[iq \sum_{r=1}^{k-1} d_{r,j}^2 \right].$$

The scattering power $f_k(q)$ of k th atomic plane is given by

$$f_k(q) = f_M(q) + f_O(q) \exp(iqd_{MO}), \quad (\text{A4})$$

where $f_M(q)$ and $f_O(q)$ are the in-plane structure factors of a certain metal and oxygen, respectively. The d_{MO} is the distance between a metal and oxygen positions in the same plane. The structure factors are given by

$$f(q) = \exp[-B \sin^2\Theta / \lambda^2] [f^0(q) + f' + if''], \quad (\text{A5})$$

where B is the Debye-Waller coefficient,²⁷ $f(q)$ is the atomic scattering factor, f' and f'' are anomalous dispersion corrections, and the in-plane scattering power $f^0(q)$ for metals is defined by

$$f_{\text{Bi}}^0(q) = (1 - \eta_{\text{Sr}} - \eta_{\text{Ca}}) f_{\text{Bi}}^0 + \eta_{\text{Sr}} f_{\text{Sr}}^0 + \eta_{\text{Ca}} f_{\text{Ca}}^0,$$

$$f_{\text{Sr}}^0(q) = (1 - \eta_{\text{Bi}} - \eta_{\text{Ca}}) f_{\text{Sr}}^0 + \eta_{\text{Bi}} f_{\text{Bi}}^0 + \eta_{\text{Ca}} f_{\text{Ca}}^0, \quad (\text{A6})$$

$$f_{\text{Ca}}^0(q) = (1 - \eta_{\text{Bi}} - \eta_{\text{Sr}}) f_{\text{Ca}}^0 + \eta_{\text{Bi}} f_{\text{Bi}}^0 + \eta_{\text{Sr}} f_{\text{Sr}}^0,$$

where η_{Bi} , η_{Sr} , and η_{Ca} are an in-plane atomic density and f_{Bi}^0 , f_{Sr}^0 , and f_{Ca}^0 are the atomic scattering powers of Bi, Sr, and Ca, respectively. Values for the atomic scattering factors were taken from Ref. 28. The scattering intensity is given by

$$I(q) = \langle F(q) F^*(q) \rangle. \quad (\text{A7})$$

It is assumed that the interlayer $d_{\text{Bi},j}$ and interplanar $d_{r,j}$ distances vary in a continuous manner. Choosing a Gaussian distribution of the $d_{\text{Bi},j}$ around the average value d_{Bi} with a width σ and of the $d_{r,j}$ around d_r with a width Δ , the scattering intensity, by averaging the intensity over these distributions, can be written^{11,29}

$$I(q) = 2M(\langle FF^* \rangle + \text{Re}[e^{\xi} \Phi \bar{F}]) + \sum_{r=1}^{M-1} (M-r) \text{Re}[2e^{2r\xi} \Phi \bar{F} T^{2r-1} + e^{(2r-1)\xi} \Phi \bar{F} T^{2r}], \quad (\text{A8})$$

where

$$\begin{aligned} \xi &= iq d_{\text{Bi}} - \frac{q^2 \sigma^2}{2}, \\ \bar{F} &= \sum_{j=1}^3 P_j \langle F_j \rangle, \\ \Phi &= \sum_{j=1}^3 P_j \langle \exp(iqc_j) F_j^* \rangle, \\ T &= \sum_{j=1}^3 P_j \langle \exp(iqc_j) \rangle, \\ \sum_{j=1}^3 P_j &= 1, \end{aligned} \quad (\text{A9})$$

and where P_j is the Gaussian probability of occurrence, c_j is the c -axis parameter, and F_j is the structure factor for Bi-2201 ($j=1$), Bi-2212 ($j=2$), and Bi-2223 ($j=3$) structures, respectively. Such a model allows us to vary the amount of the randomly distributed stacking faults in the film by altering P_1 , P_2 , and P_3 .

Finally, the intensity scattered by a Bi-2212 film with the absorption and the Lorentz-polarization factors can be written as

$$I_c(q) = \left[1 - \exp\left[-\frac{2\mu\tau}{\sin\Theta}\right] \right] \frac{1 + \cos^2 2\Theta}{\sin 2\Theta} K I(q), \quad (\text{A10})$$

where μ is the absorption coefficient, τ is the total thickness of the film and K is the scaling factor. To allow a quantitative comparison between the described model and the measured profiles, the standard minimizing function of the Numerical Algorithms Group library was used.³⁰ As fitting parameters, the interplanar distances between BiO, SrO, and CuO₂ planes with the continuous distance fluctuations and the in-plane atomic substitutions of Bi, Sr, and Ca were used. The value of χ^2 given by²⁴

$$\chi^2 = \frac{\sum_{i=1}^{N_{\text{pt}}} \{ [I_c(i) - I_m(i)]^2 / I_m(i) \}}{\sum_{i=1}^{N_{\text{pt}}} I_m(i)}, \quad (\text{A11})$$

was minimized, where N_{pt} is the number of points in the profile and I_c and I_m are the calculated and measured x-ray intensities, respectively.

- ¹H. Maeda, Y. Tanaka, M. Fukutomi, and T. Asano, *Jpn. J. Appl. Phys.* **27**, L209 (1988).
²M. A. Subramanian, C. C. Torardi, J. C. Calabrese, J. Gopalakrishnan, K. J. Morrissey, T. R. Askew, R. B. Flippen, U. Chowdry, and A. W. Sleight, *Science* **240**, 631 (1988).
³V. Petricek, Y. Gao, P. Lee, and P. Coppens, *Phys. Rev. B* **42**, 387 (1990).
⁴A. Yamamoto, M. Onoda, E. Takayama-Muromachi, and F. Izumi, *Phys. Rev. B* **42**, 4228 (1990).
⁵For a review, see, S. Uchida, *Jpn. J. Appl. Phys.* **32**, 3784 (1993).
⁶H. Zhang and H. Sato, *Phys. Rev. Lett.* **70**, 1697 (1993).
⁷R. J. Cava, *Science* **247**, 656 (1990).
⁸G. S. Grader, E. M. Gyorgy, P. K. Gallagher, H. M. O'Bryan, D. W. Johnson, Jr., S. Sunshine, S. M. Zahurak, S. Jin, and R. C. Sherwood, *Phys. Rev. B* **38**, 757 (1988).
⁹K. Tanaka, H. Takaki, and S. Mizuno, *Jpn. J. Appl. Phys.* **31**, 2692 (1992).
¹⁰S. A. Sunshine, T. Siegrist, L. F. Schneemeyer, D. W. Murphy, R. J. Cava, B. Batlogg, R. B. van Dover, R. M. Fleming, S. H. Glarum, S. Nakahara, R. Farrow, J. J. Krajewski, S. M. Zahurak, J. V. Waszczak, J. H. Marshall, P. Marsh, L. W. Rupp, Jr., and W. F. Peck, *Phys. Rev. B* **38**, 893 (1988).
¹¹E. E. Fullerton, I. K. Schuller, H. Vanderstraeten, and Y. Bruynseraede, *Phys. Rev. B* **45**, 9292 (1992).
¹²A. Brazdeikis, A. Vailionis, and A. Flodström, *Applied Superconductivity*, edited by H. C. Freyhardt (DGM Informationsgesellschaft GmbH, Oberursel, 1993), p. 563.
¹³A. Brazdeikis, C. Tracholt, A. Vailionis, and A. S. Flodström (unpublished).
¹⁴By introducing the continuous interplanar distance fluctua-

tions, only broadening of the Bragg peaks is obtained. The presence of stacking faults may alter the shape and the positions of the peaks. In the experimental XRD spectra, different Bragg peaks exhibit different linewidths which can be caused only by the presence of stacking faults. A small proportion of stacking faults (less than 10%) does not greatly influence the peak intensities, and therefore other factors must be considered.

- ¹⁵See, for instance, P. Wagner, F. Hillmer, U. Frey, H. Adrian, T. Seibold, L. Ranno, A. Elschner, I. Heyvaert, and Y. Bruynseraede, *Physica C* **215**, 123 (1993); J. Auge, U. Rüdiger, H. Frank, H. G. Roskos, G. Güntherodt, and H. Kurz, *Appl. Phys. Lett.* **64**, 378 (1994), and references therein.
¹⁶L. M. Rubin, T. P. Orlando, and J. B. Vander Sande, *Physica C* **220**, 284 (1994).
¹⁷G. Poullain, R. Desfeux, and H. Murray, *Physica C* **214**, 195 (1993).
¹⁸I. Bozovic, J. N. Eckstein, M. E. Klausmeier-Brown, and G. Virshup, *J. Supercond.* **5**, 19 (1992).
¹⁹D. G. Schlom, A. F. Marshall, J. T. Sizemore, Z. J. Chen, J. N. Eckstein, I. Bozovic, K. E. von Dessionneck, J. S. Harris, Jr., and J. C. Bravman, *J. Cryst. Growth* **102**, 361 (1990).
²⁰Y. Nakayama, I. Tsukada, and K. Uchinokura, *J. Appl. Phys.* **70**, 4371 (1991).
²¹S. Yokoyama, T. Ishibashi, M. Yamagami, and M. Kawabe, *Jpn. J. Appl. Phys.* **30**, L106 (1990).
²²Different pieces of the same as-grown films were annealed at 360 °C for different times ranging from 1 to 6 h. The temperature-dependent resistivity data showed an increase in $T_{c, \text{zero}}$ from 55–60 to 70 K and further decrease to 50 K with longer annealing times. XRD data indicated that, with the

- accuracy of the experiment, the c -axis lattice constant remained the same for the film with a maximum $T_{c,zero}$ of 70 K and decreased slightly at longer annealing times. These results can be interpreted as indicating that the critical temperature, $T_{c,zero}$ is affected by a redistribution of oxygen, i.e., that the hole carrier density needs to be optimized, although the broad transition character still remained.
- ²³B. E. Warren, *X-ray Diffraction* (Addison-Wesley, Reading, MA, 1969), p. 251.
- ²⁴*The Rietveld Method*, edited by R. A. Young (Oxford University Press, New York, 1993), pp. 22 and 132.
- ²⁵S. N. Putilin, E. V. Antipov, and M. Marezio, *Physica C* **212**, 266 (1993).
- ²⁶*Thallium-based High-temperature Superconductors*, edited by Allen M. Herman and J. V. Yakhmi (Marcel-Dekker, New York, 1994), p. 26.
- ²⁷*Chemistry of Superconductor Materials*, edited by T. A. Vanderah (Noyes, New Jersey, 1992), p. 506.
- ²⁸*International Tables for X-ray Crystallography III* (Kynoch, Birmingham, 1974), p. 99.
- ²⁹I. S. Gradshteyn and I. M. Ryzhik, *Tables of Integrals, Series and Products* (Academic, New York, 1963), p. 307.
- ³⁰*The NAG Fortran Library Manual* (Numerical Algorithms Group, Oxford, 1987).